Tribol Lett (2015) 57:12
DOI 10.1007/s11249-014-0459-0

ORIGINAL PAPER

Tribological Behavior of Sandwich-Like Self-Assembled Films Containing Silver Nanoparticles: The Influence of Outer Molecular Structure and Chain Length

Guangbin Yang · Fengjie Jin · Laigui Yu · Pingyu Zhang

Received: 3 July 2014 / Accepted: 22 December 2014 / Published online: 11 January 2015

Abstract Alkanethiols with different chain length, composition and structure were grafted onto the surface of 3-mercaptopropyl trimethoxy silane (MPTS)–Ag dual-layer film consisting of Ag outerlayer and MPTS underlayer, thereby generating self-assembled trilayer films with "sandwich" structure on Si substrate. As-prepared films were characterized by atomic force microscopy and X-ray photoelectron spectroscopy. Moreover, the tribological behavior of as-prepared films was evaluated with an atomic force microscope and a ball-on-plate tribometer as well. It was found that as-prepared MPTS–Ag–C12 (C12 refer to 12 carbon chain of alkyl mercaptan; the same hereafter) film possesses excellent friction-reducing and antiwear properties. Particularly, MPTS–Ag–C8F (C8F refers to perfluorooctanethiol) film with lower interfacial energy exhibits a longer antiwear life than MPTS–Ag–C8 film.

Keywords Self-assembly · Ag nanoparticles · "Sandwich" structure · Tribological properties

1 Introduction

Tribological properties in nano- and microscales between two sliding solid surfaces have drawn much attention as they significantly affect the performance of microdevices such as microelectromechanical systems (denoted as MEMS) and nanoelectromechanical systems (denoted as NEMS) [1, 2]. Besides, they can provide crucial information for understanding fundamental mechanism and origin of friction and wear [3, 4]. It is usually expected that surfaces and interfaces with low adhesion and friction can alleviate adhesion and friction issues at small scales [3]. Since friction and wear in the boundary lubrication conditions are governed by the properties of the solid surfaces and boundary lubricant films other than bulk viscosity [5], the design of surfaces and interfaces with low adhesion and friction is increasingly attracting attention and playing important role in the development of MEMS/NEMS [2–4].

In order to resolve the friction-related problems, tribologists have resorted to a variety of surface modification techniques to mitigate forces such as friction and adhesion in MEMS [5]. Under such conditions, self-assembled monolayers (denoted as SAMs) as ideal molecular lubricants for MEMS have attracted much attention in past years [5, 6], owing to their properties such as thermodynamic stability, formation of close packed structures, hydrophobicity and strong bonding (chemisorption) to the substrates [5, 7]. In addition, extensive discussions have appeared in the literature addressing the details of friction at the molecular level, especially with regard to determining the relationship between adhesion and friction [8].

Although SAMs could significantly reduce friction and wear on surfaces under low loads with minimal contact, these single-layer films are generally insufficient for mitigating wear under high loads and continuous shearing, due to rapid breakdown under high pressures. Strategies beyond simple, single-component SAMs are thus necessary to meet the needs of contact lubrication in MEMS and other devices [9]. Ma et al. [10] proposed multicomponent-based SAMs composed of self-assembled films paired with weakly bound molecules as mobile lubricants to replenish the lubricant coating when the SAMs fail for MEMS lubrication. To improve the load carrying abilities of the film, Song [11] and Ou [12] separately constructed bilayer

G. Yang · F. Jin · L. Yu · P. Zhang (✉)
Key Laboratory of Ministry of Education for Special Functional Materials, Henan University, Kaifeng 475004, China
e-mail: yang0378@henu.edu.cn; pingyu@henu.edu.cn

and trilayer organic films on silicon wafer. Furthermore, graphene oxide was also introduced in self-assembled films to design trilayer films which possess good friction-reducing and antiwear properties because of its intrinsic structure [13–15].

Metal Ag is soft and malleable, and it is a traditional solid lubricating material. In recent years, with the development of nanotechnology, Ag nanoparticles as a solid lubricating material have received intensive attention, because they are cost-effective (compared with gold) and stable in air (compared with copper and nickel) and exhibit excellent friction-reducing and antiwear abilities in films [16, 17], composite materials [18] and as lubricant additives as well [19].

In the previous studies, we found that sandwich-like self-assembled *n*-octanethiol film containing silver nanoparticles exhibits attractive friction-reducing and antiwear properties, because of its peculiar sandwich-like structure. In particular, its outmost molecular chain with significant freedom of swing allows rearrangement along the sliding direction under shear stress, thereby eventually resulting in a smaller resistance and lower friction values during sliding [20]. In the present research, alkanethiols with different chain length, composition and structure were grafted onto the surface of 3-mercaptopropyl trimethoxy silane (MPTS)–Ag dual-layer film composed of Ag outerlayer and MPTS underlayer to form trilayer films with "sandwich" structure on Si substrate. This paper reports the tribological behavior of as-prepared films as well as the effects of the alkyl chain length and molecular structure on the tribological behavior of the films.

2 Experiment Section

2.1 Materials

A single-crystal silicon wafer (1 0 0) which was polished on one side was used as substrate for preparing self-assembled trilayer films with "sandwich" structure. Analytical grade reagents *n*-octanethiol, *n*-dodecanethiol, *n*-hexadecanethiol and MPTS were provided by Alfa Aesar China (Tianjin, China) Company Ltd 1H,1H,2H,2H-perfluorooctanethiol was obtained form Aldrich, and analytically pure silver nitrate and polyvinyl pyrrolidone (denoted as PVP) were supplied by Tianjin Kermel Chemical Reagent Company Ltd and BASF (Germany), respectively. All other chemicals used in chemical manipulations are of reagent grade. All the reagents were used without further purification.

Deionized water (>18 MΩcm, Millipore Milli-Q) was used for preparation of all aqueous solutions and for rinsing as well.

2.2 Synthesis and Characterization of Ag Nanoparticles

Ag nanoparticles were prepared according to the literature [20], and their structure was characterized with a JEM-2010 transmission electron microscope (TEM; accelerating voltage: 200 kV) and a dynamic light scattering (DLS) system. Briefly, 0.1359 g of PVP and 40 mL of deionized water were placed in a 250-mL flask which was equipped with a magnetic stirrer. Resultant mixed solution was stirred and heated to 70 °C. Then, a solution of $AgNO_3$ (0.4077 g) in deionized water (30 mL) and 5 mL of ethanol were sequentially added into the flask and allowed to react at 70 °C for 2 h before cooling down to room temperature. When the reaction solution turns from colorless to light orange, silver nanoparticles were produced.

2.3 Preparation of Ag-Containing Self-Assembled Trilayers

Silicon substrates (1 0 0) were first immersed in Piranha solution (98 % H_2SO_4: 30 % H_2O_2 = 7: 3 v/v) at 90 °C for 30 min to generate hydroxyl radicals on the surfaces, followed by a thorough rinsing in deionized water and drying with flowing N_2 to obtain a fresh and clean surface. The pretreated silicon wafers were subsequently immersed in a 10 mM MPTS solution in isopropanol–water (5:1 v/v) for 15 h. Then, the wafers were taken out and cleaned with isopropanol and deionized water, followed by drying with flowing N_2 affording film sample denoted as MPTS SAM.

The MPTS SAM-modified silicon substrates were put into a freshly prepared solution of 10 mM Ag nanoparticles and kept for 4 h. After being removed from the Ag nanoparticles solution, the samples were rinsed in deionized water and dried with flowing N_2 to afford film sample denoted as MPTS–Ag.

As-obtained silicon wafers with MPTS–Ag film were immersed in 20 mmol/L *n*-octanethiol (or *n*-dodecanethiol or *n*-hexadecanethiol or perfluorooctanethiol) alcohol solution for 15 h at room temperature and then taken out from the solution, followed by washing in alcohol and deionized water and drying with flowing N_2 to afford film samples denoted as MPTS–Ag–C_x (x = 8, 12, 16; referring to the carbon chain of alkanethiols) and MPTS–Ag–C8F (C8F refers to perfluorooctanethiol). There exist strong chemical interactions between the mercapto group and silver metal in MPTS–Ag–C_x trilayer film. The schematic representation of trilayer MPTS–Ag–C_x films with "sandwich-like" structure is shown in Fig. 1.

2.4 Characterization

The chemical states of the interesting elements in the self-assembled films were determined with a multi-functional

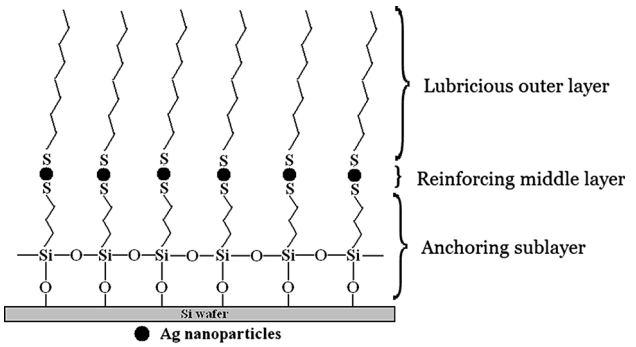

Fig. 1 Schematic representation for the preparation of trilayer self-assembled films with "sandwich-like" structure on silicon wafer

X-ray photoelectron spectroscope (XPS; monochromated Al K_α radiation, power 150 W, pass energy 40 eV). XPS analysis was conducted at a chamber pressure of $\sim 3 \times 10^{-8}$ torr, and the binding energy of contaminated carbon (C1 s: 284.8 eV) was used as a reference.

The surface morphologies of different samples were observed with an SPA400 atomic force microscope (AFM, Seiko Inc., Japan) in tapping mode while commercial silicon microcantilever probes were used. The tip radius and spring constant are <50 nm and 2.0 N/m, respectively.

The static contact angles of deionized water on various film samples were measured with a DropMaster 300 solid/liquid interface analyzer (Kyowa Interface Science, Japan). The average values of at least five repeat measurements for each sample were obtained.

2.5 Evaluation of Macro- and Micro-Tribological Behaviors of Various Films

The micro-friction and adhesion of the self-assembled trilayer films were evaluated also using the SPA400 AFM, which was carried out in a contact mode (scan distance 2 μm, scan angle 90°, scan rate 1.2 Hz, normal force 20 nN). Commercially available Al-coated V-shaped Si_3N_4 cantilever and a Si_3N_4 tip thereon with a radius of <20 nm and a spring constant of 2.0 N/m were used for the measurements. The output voltages were directly used as the relative friction forces. Friction force loops were obtained from at least five separate locations on each sample surface. Force–distance measurements with the AFM were used to measure the adhesion force between the film surfaces and the AFM probe tip. For all measurements, the same cantilever was used, and no attempt was made to calibrate the torsional force constant. All the tests were conducted at a room temperature of 25 °C and a relative humidity of 50 %.

The macro-tribological behavior of the self-assembled films was evaluated using a UMT-2 tribometer (CETR) in a ball-on-plate contact configuration. Commercially available 440C stainless steel ball (4 mm in diameter) was used as the stationary upper counterpart, whereas the lower tested sample was mounted onto the flat base and driven to slide reciprocatively at a distance of 5 mm. Friction was measured at an applied normal load of 0.5 N and a sliding speed of 300 mm/min. The friction coefficient versus sliding time curves were recorded automatically. At least five repeat measurements were performed for each frictional pair. The failure of the self-assembled films is assumed to occur when the friction coefficient rises sharply to a high and stable value similar to that of a clean silicon against the same counterpart (about 0.65), and the sliding time at this point is recorded as the antiwear life of the tested self-assembled trilayer films. All the friction and wear tests were performed at room temperature and in ambient air.

The surface morphology of the wear tracks of the films were observed with a Nova NanoSEM 450 field emission scanning electron microscope (FESEM).

3 Results and Discussion

3.1 Characterization of Ag Nanoparticles

The typical TEM image of as-synthesized Ag nanoparticles is shown in Fig. 2a. It can be seen that Ag nanoparticles are of uniform spherical shape and have a narrow size distribution (most of the particles have an average size of about 3–5 nm), while they tend to be free of agglomeration. The size distribution of Ag nanoparticles determined by DLS is shown in Fig. 2b. As-synthesized Ag nanoparticles have a mean particle diameter of 7.5 nm and show nearly normal size distribution. The size of Ag nanoparticles determined by DLS is much larger than that estimated from TEM image, mainly because DLS measurements take the hydrodynamic radius of the organic surface-capping agent around the nanoparticles into account [21].

3.2 Characterization of Films

Figure 3 shows the XPS spectra acquired from the MPTS–Ag–C8 and MPTS–Ag–C8F coated silicon substrates. In Fig. 3a, there are two peaks symmetrically centered at 368.5 eV and 374.4 eV corresponding to $Ag3d_{5/2}$ and $Ag3d_{3/2}$, respectively. The spin energy separation is about 6.0 eV, indicating that the silver species deposited in the film MPTS–Ag–C8 are in form of metallic nature [22]. The S2p signal in the spectrum for the modified silicon substrate can qualitatively account for the existence of MPTS or alkanethiols on silicon surface. The S2p peak is symmetric and centered around 163.8 eV, which indicates that MPTS or alkanethiols films have been successfully

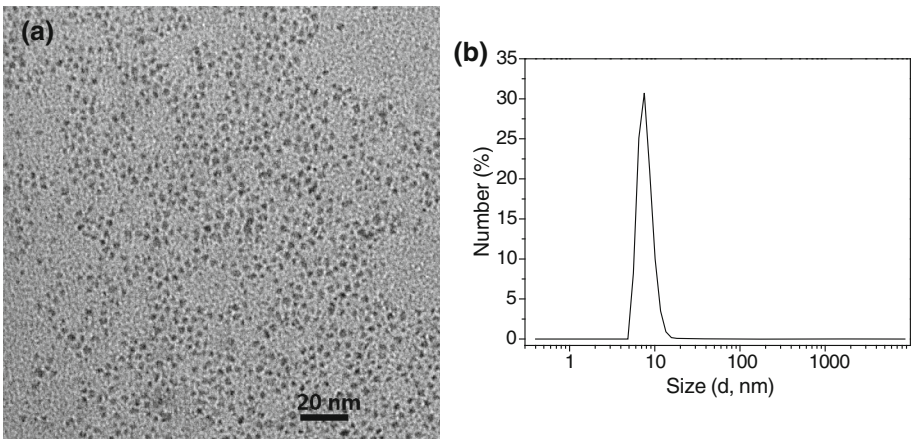

Fig. 2 **a** TEM image and **b** size distribution of as-synthesized Ag nanoparticles

obtained in our work, as shown in Fig. 3b. Except for MPTS–Ag–C8F, other films have the same XPS results as MPTS–Ag–C8. As to MPTS–Ag–C8F, it adds a peak of F 1s, namely the F 1s peak at 689.0 eV (Fig. 3c) demonstrates that Ag nanoparticles-doped MPTS SAMs have been successfully modified by perfluorooctanethiol.

As we know, AFM is an increasingly popular technique to assess film roughness and morphology. Figure 4 shows typical tapping-mode three-dimensional AFM images of MPTS–Ag–C_x ($x = 8$, 12 and 16; the same hereafter) and MPTS–Ag–C8F. As shown in Fig. 4a, c, d, the MPTS–Ag–C_x films are compact and have similar morphology, and they have a small size distribution as well. Besides, MPTS–Ag–C_x films are packed closely and have few defects, which is of great importance for the protection of the underlying surface. Furthermore, they are homogenous and relatively smooth (their root mean surface roughness, abbreviated as RMS, over a scan range of 5 μm × 5 μm is 1.80 nm ($x = 8$), 1.05 nm ($x = 12$) and 1.57 nm ($x = 16$), respectively. Moreover, the surface of the MPTS–Ag–C8F film is rougher and looser than that of MPTS–Ag–C8 film, and the former has a bigger particle size and a broader size distribution as well than the latter (the RMS roughness of MPTS–Ag–C8F film is increased to 3.77 nm (Fig. 4b).

Water contact angle (abbreviated as WCA) measurement is simple, useful and sensitive for gaining insight into surface chemical components. As depicted in Table 1, the WCA of MPTS–Ag–C_x is about 45°, and it undergoes insignificant change with increasing alkyl chain length of alkanethiols. It means that the chain length of alkanethiols does not significantly affect the surface energy of MPTS–Ag–C_x films. However, the WCA increases to 109.5° when perfluorooctanethiol is capped on the surface of MPTS–Ag films. Such a significant change in the WCA of MPTS–Ag–C8F film indicates that the modification of MPTS–Ag films by perfluorooctanethiol in our work is successful, thereby leading to the reduction of the surface energy [23].

3.3 Tribological Behavior

3.3.1 Micro-Tribological Behavior

The micro-tribological behavior of the self-assembled films was evaluated with an AFM at a normal load of 20 nN. A representative plot of the friction forces (F_L; expressed as voltage signals) versus the lateral displacement of MPTS–Ag–C12 is shown in Fig. 5. The upper and lower curves indicate the trace and retrace friction force profiles, respectively. The fluctuation of the profile seems to be attributed to the roughness of the MPTS–Ag–C12-coated Si substrate [24]. As shown in Fig. 5, the MPTS–Ag–C12 has a friction force of about 800 mV. The micro-friction forces of various film samples under the same applied load are also summarized in Table 1. The friction force loops at a distance of 2.0 μm were obtained from different regions. From Table 1, it can be seen that the friction force of the MPTS–Ag–C_x films tends to decrease with the increase of carbon backbone chain length up to 12 carbon atoms ($x = 12$), namely MPTS–Ag–C12 shows a lower friction force than MPTS–Ag–C8, which is possibly attributed to the different packing density of dodecanethiol molecules. In other words, as the carbon backbone chain length rises up to 12 carbon atoms, the intermolecular interactions are enhanced, and the dodecanethiol molecules are packed more densely, thereby decreasing the energy dissipation during sliding and finally resulting in a lower friction force [25]. Furthermore, we speculate that the longer molecule chain ($x = 12$) exhibits more flexibility than the shorter molecule chain ($x = 8$), which also contributes to reducing friction force. Similar relationship between the chain length and friction force of SAMs is also reported elsewhere [26]. However, MPTS–Ag–C16 with longer hydrocarbon chain shows a slightly higher friction force than MPTS–Ag–C12 with a relatively shorter hydrocarbon chain. This can be explained in terms of the rigidity of

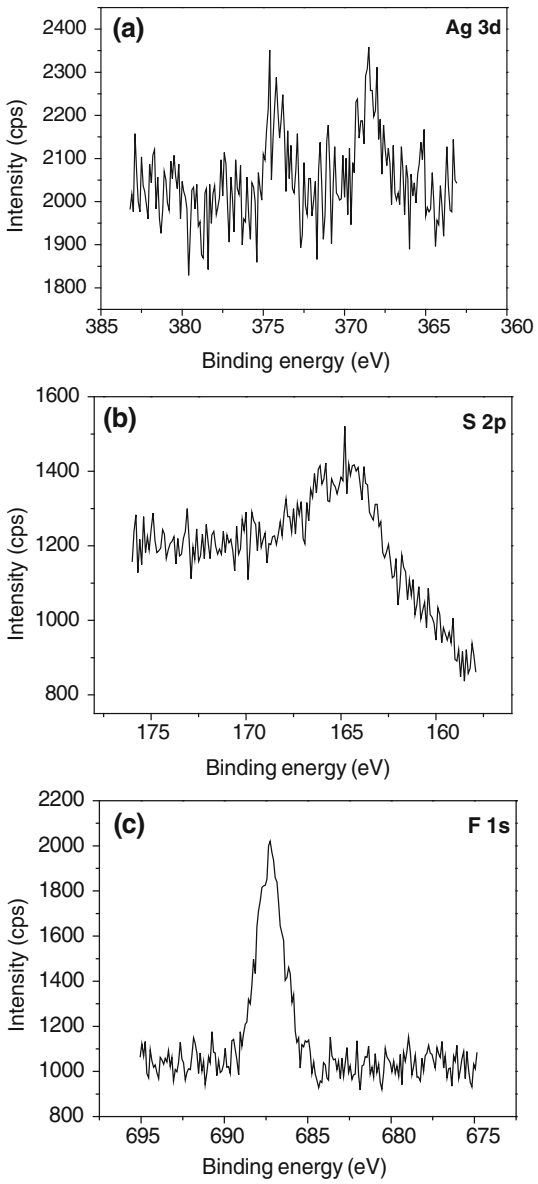

Fig. 3 XPS spectra of **a** Ag 3d, **b** S 2p for MPTS–Ag–C8 and **c** F 1s for MPTS–Ag–C8F self-assembled trilayer

SAM. When the room temperature is lower than 18 °C, the hydrocarbon chain of dodecanethiol is expected to be in a fluid-like state, whereas that of hexadecanethiol is in a frozen state because of the stronger lateral cohesion among chains. The fluid-like chains are more compliant and thus give a smaller resistance to shear [24]. In addition, MPTS–Ag–C8F exhibits better antiwear ability than MPTS–Ag–C8. The reason lies in that the backbone structure of perfluorinated carbon chains is harder to rotate (due to the different sizes of F atom vs. H atom) than common carbon chains. In other words, the molecular structure of C8F is more rigid than that of C8 [27], since the C–C bond strength increases when hydrogen is replaced with fluorine [28]. Therefore, the rigid perfluorinated carbon backbone may be responsible for the increased antiwear ability of MPTS–Ag–C8F film.

Adhesion force was measured from the force–distance curve recorded with AFM [23]. Figure 6 shows the force–distance curve recorded from MPTS–Ag–C12 film. The tip initially experiences an attractive force when it gradually approaches to the sample. As the tip further approaches to the sample, the normal force eventually turns repulsive and results in an upward cantilever deflection as a small normal force is applied to the sample surface. Then, the cantilever begins to retract. The tip goes beyond the zero deflection (flat) line, due to adhesion forces. The magnitude of the cantilever deflection equals to the adhesion force. Finally, the cantilever snaps back and shows zero deflection, and this point is also called the "pull off" point at which the cantilever pulls off from the sample and the adhesion force is thus called the "pull off" force. The adhesion forces of the other self-assembled trilayer films were also measured by AFM, and relevant measured adhesion forces are summarized in Table 1. The adhesion force of MPTS–Ag–C12 film is about 1.2 μN, and it is higher than those of the other two MPTS–Ag–C_x ($x = 8$ and 16) films. Furthermore, MPTS–Ag–C8F shows a lower adhesion value of about 0.6 μN than MPTS–Ag–C8 (1.0 μN) owing to its lower interfacial energy indicated by its higher water contact angle (109.5°). It is well known that the adhesion force arises from various attractive forces such as capillary, electrostatic, van der Waals and chemical bonding. Among these forces, the capillary force produced by condensation of adsorbed water or lubricant is the strongest, thus the contribution of capillary force to the adhesion force should be significant [29, 30]. When the surface is hydrophilic, meniscus will be easily formed by adsorbing water molecules in air, causing a higher adhesion force [31]. With increasing alkyl chain length of alkanethiols, the WCA of relevant self-assembled films undergoes few changes, which implies that the contribution of capillary force to the adhesion force should be almost the same. Furthermore, the self-assembled film of short-chain molecule has small van der Waals force, so MPTS–Ag–C8 film is inferior to MPTS–Ag–C12 film in terms of the adhesion force [32]. Moreover, the molecule structure of C16 in MPTS–Ag–C16 film is the most rigid among the three kinds of carbon chains under investigation, and hence MPTS–Ag–C16 film exhibits very low adhesion force.

3.3.2 Macro-Tribological Behavior

The macro-tribological behaviors of the self-assembled trilayer films were evaluated with a ball-on-plate UMT-2 tribometer at a normal load of 0.5 N and an invariable sliding speed of 300 mm/min, and the results are presented in Fig. 7. MPTS–Ag–C8 film has an antiwear life of

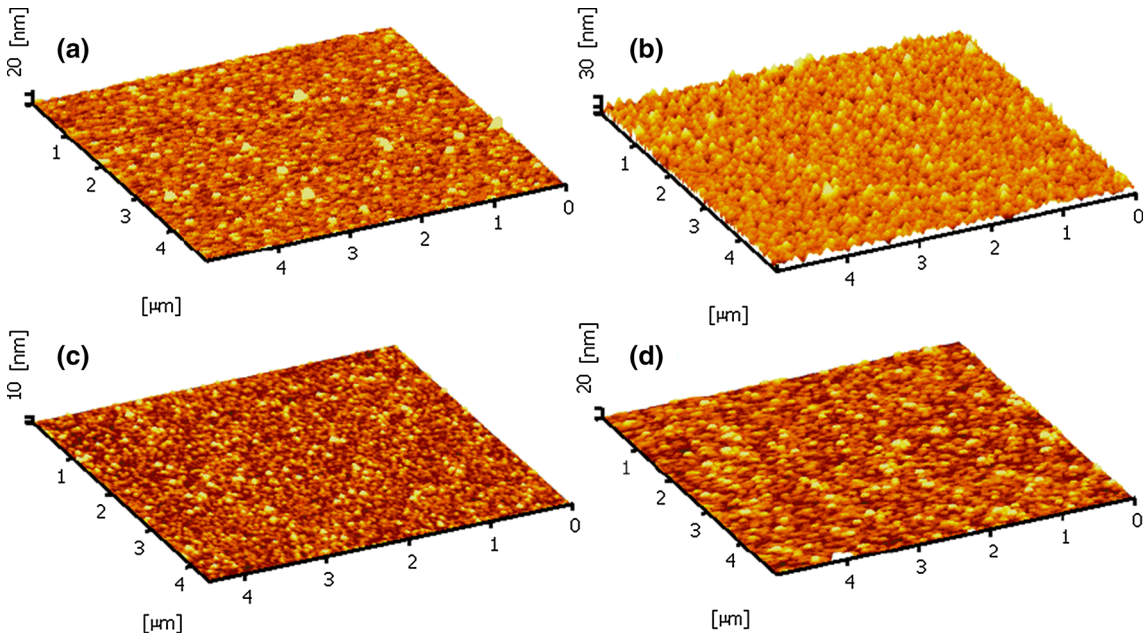

Fig. 4 Three-dimensional AFM images of **a** MPTS–Ag–C8, **b** MPTS–Ag–C8F, **c** MPTS–Ag–C12 and **d** MPTS–Ag–C16

Table 1 Characterization of self-assemble films

Test sample	RMS (nm)	Water contact angle (degree)	Adhesion (μN)	Micro-friction (mV)
MPTS–Ag–C8	1.80	44.7	1.0	1,034
MPTS–Ag–C8F	3.77	109.5	0.6	616
MPTS–Ag–C12	1.05	49.8	1.2	794
MPTS–Ag–C16	1.57	42.7	0.8	887

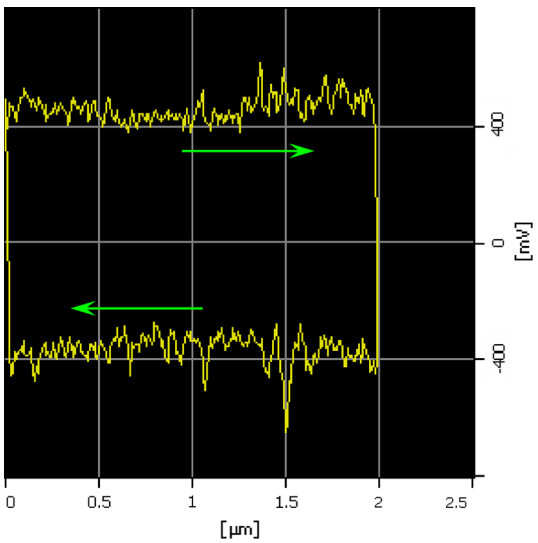

Fig. 5 Frictional curves of MPTS–Ag–C12 film

32,000 s. MPTS–Ag–C12 film shows an antiwear life of above 40,000 s, while MPTS–Ag–C16 film under the same condition exhibits an antiwear life of only 17,000 s. On one hand, with the increase in alkyl chain length of MPTS–Ag–C_x ($x = 8$, 12), the intermolecular force rises, and the orderliness and compactness of the self-assembled films increase, thereby resulting in a long antiwear life [9]. On the other hand, reduction in friction coefficients caused by increasing the chain length may be attributed to the increased lateral cohesive interactions between the adsorbed molecules [33]. These cohesive forces arise from intermolecular chain dispersion forces, which depend on the number of methylene groups on the adsorbed molecules. Therefore, surface films containing longer chain length molecules would be more resistant to disruption by the higher temperatures and pressures at the asperity contacts. Hence, the antiwear life would be longer. As indicated by previous reports, a long chain molecule tends to form a densely packed monolayer with less surface defects. We speculate that it was the longer molecule chain with more flexibility that was responsible for lower friction coefficient [34]. Interestingly, corresponding to relevant AFM data shown in Fig. 6, as the carbon number of outer chain length increases from 12 to 16, the antiwear life of MPTS–Ag–C16 film decreases, which agreed with what

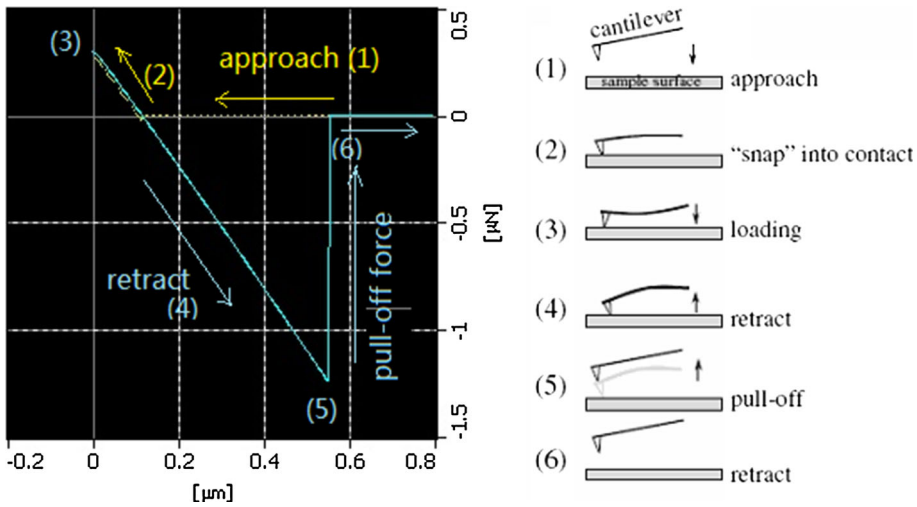

Fig. 6 Force–distance curves of MPTS–Ag–C12 film

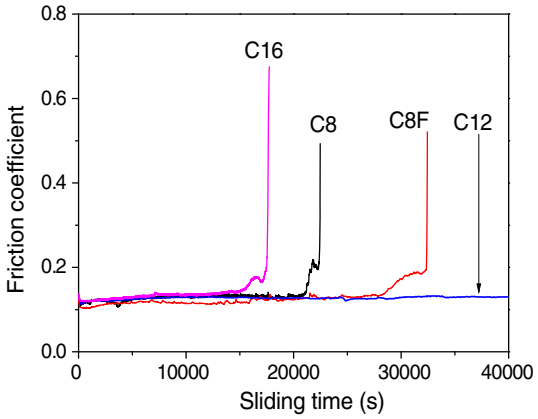

Fig. 7 Variations of friction coefficients with sliding time for self-assembled films sliding against stainless steel ball at 300 mm/min under a normal load of 0.5 N

was reported elsewhere [25]. Such a phenomenon could be explained as follows. As the carbon chain length increases to 16 at a room temperature of lower than 18 °C, hexadecanethiol molecule is in a frozen state, which could readily cause microstructure defect and increase the energy dissipation during sliding. As a result, antiwear life decreases as chain length increases to 16. In addition, MPTS–Ag–C8F film exhibits a longer antiwear life than MPTS–Ag–C8 film, because improving surface hydrophobicity can reduce water adsorption, and hence reduce meniscus-mediated adhesion and friction forces between contacting surfaces [35]. In other words, since the MPTS–Ag–C8F film with a stronger hydrophobicity has a lower surface energy, as evidenced by the contact angle measurement, it should have a lower adhesion force to the steel ball than MPTS–Ag–C8 film, thus it exhibits lower friction coefficient and longer antiwear life [36].

3.3.3 SEM Analysis of Wear Tracks

To understand the effect of alkyl chain length of alkylthiols and molecular structure on the tribological behavior of self-assembled films, we observed the worn surfaces of MPTS–Ag–C_x films and MPTS–Ag–C8F film with SEM. Figure 8 shows the representative SEM images of the wear tracks tested at a normal load of 0.5 N and a sliding speed of 300 mm/min. The worn surface of MPTS–Ag–C8 film sliding against the stainless steel ball for 22,000 s shows signs of severe plastic deformation and contains numerous wear debris (Fig. 8a), which corresponds to its high friction coefficient and short antiwear life. The wear track of MPTS–Ag–C8F film shows signs of mild scuffing and mild plastic deformation as well (Fig. 8b), corresponding to its good friction-reducing and antiwear abilities. The wear track of MPTS–Ag–C12 film (even after sliding against the stainless steel ball for 45,000 s) is narrower than that of MPTS–Ag–C8 film (Fig. 8c) and shows signs of slight plastic deformation, which corresponds to its lower friction coefficient and longer antiwear life. As to MPTS–Ag–C16 film, its wear track is larger and contains some grooves in association with obvious signs of adhesion (Fig. 8d), though the sliding time is reduced to 17,000 s. Due to the adhesion, the sliding between the film surface and the steel surface is transferred to that between the film and its transferred film on the counterpart surface as such an adhesion-transfer proceeds. Besides, there is some rodlike wear debris in the wear track of MPTS–Ag–C16 film, which may also correspond to its increased friction coefficient and decreased antiwear life as compared with MPTS–Ag–C12 film. The SEM results are consistent with the tribological behavior of the films, indicating that MPTS–Ag–C12 film with a moderate alkyl chain length may find promising applications in reducing friction and wear of MEMS and NEMS.

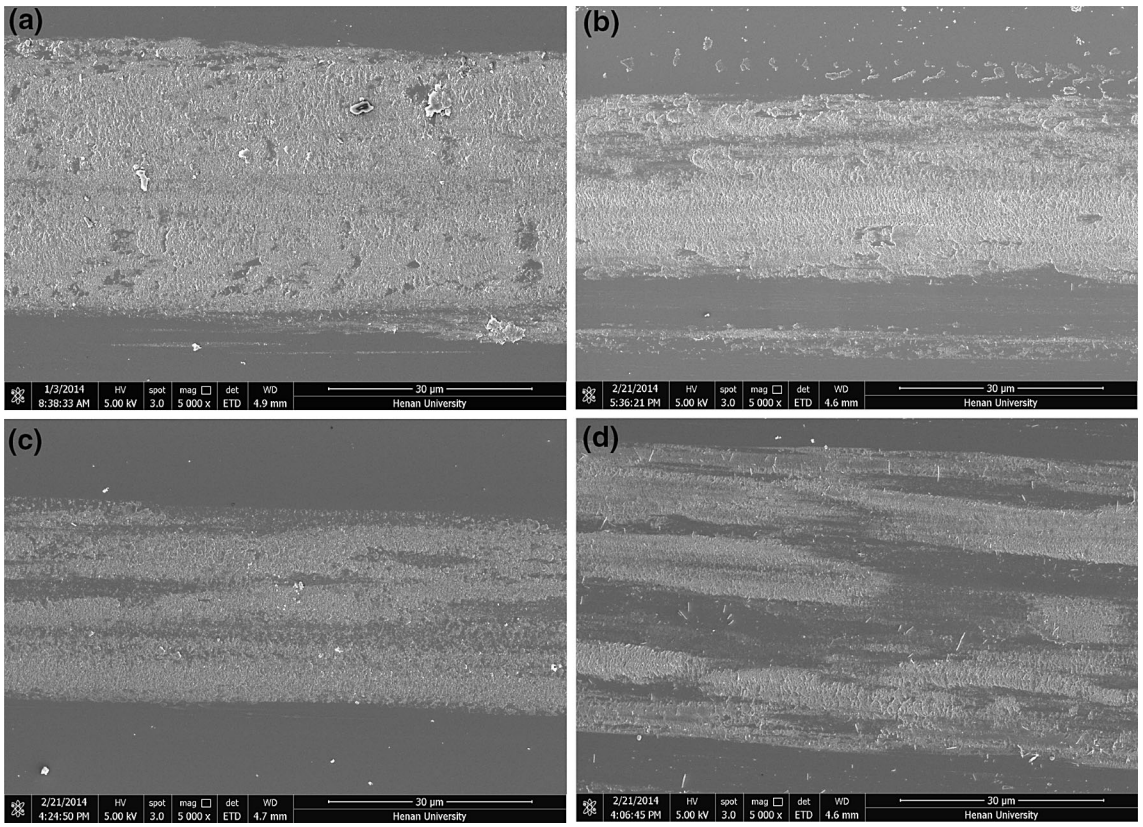

Fig. 8 SEM image of the wear tracks of **a** MPTS–Ag–C8, **b** MPTS–Ag–C8F, **c** MPTS–Ag–C12 and **d** MPTS–Ag–C16

4 Conclusions

Alkanethiols with different chain length were grafted onto the surface of Ag nanoparticle-doped 3-mercaptopropyl trimethoxy silane film to afford alkyl mercaptan/MPTS–Ag self-assembled trilayer films with "sandwich" structure on Si substrates. As-prepared trilayer SAMs exhibit superior friction-reducing and antiwear abilities and can act as effective lubricants to protect Si substrates. Although as-prepared self-assembled trilayer films with different carbon chain lengths show few differences in morphology, their tribological behavior varies significantly with varying carbon chain length of alkanethiols, due to varying intramolecular forces as well as molecular rigidity therewith. Particularly, MPTS–Ag–C12 film possesses excellent friction-reducing and antiwear abilities among various tested SAMs, showing promising potential as a low-friction and antiwear coating for MEMS or NEMS.

Acknowledgments The authors acknowledge the financial support provided by the Ministry of Science and Technology of China (project of "973" Plan, Grant No. 2013CB632303), National Natural Science Foundation of China (Grant No. 51275154), and Program for Changjiang Scholars and Innovative Research Team in University (Grant No. PCS IRT1126).

References

1. Burton, Z., Bhushan, B.: Hydrophobicity, adhesion, and friction properties of nanopatterned polymers and scale dependence for micro- and nanoelectromechanical systems. Nano Lett. **5**, 1607–1613 (2005)
2. Bhushan, B., Palacio, M., Kinzig, B.: AFM-based nanotribological and electrical characterization of ultrathin wear-resistant ionic liquid films. J. Colloid Interface Sci. **317**, 275–287 (2008)
3. Tao, Z., Bhushan, B.: Surface modification of AFM Si_3N_4 probes for adhesion/friction reduction and imaging improvement. J. Tribol. **128**, 865–875 (2006)
4. Chai, Z., Liu, Y., Lu, X., He, D.: Nanotribological behavior of ultra-thin Al_2O_3 films prepared by atomic layer deposition. Tribol. Lett. **55**, 143–149 (2014)
5. Bhushan, B.: Modern tribology handbook, vol. 2, pp. 909–929. CRC Press, Boca Raton (2001)
6. Ren, S.L., Yang, S.R., Wang, J.Q., Liu, W.M., Zhao, Y.P.: Preparation and tribological studies of stearic acid self-assembled monolayers on polymer-coated silicon surface. Chem. Mater. **16**, 428–434 (2004)
7. Maboudian, R., Howe, R.T.: Critical review: adhesion in surface micromechanical structure. J. Vac. Sci. Technol., B **15**, 1–20 (1997)
8. Houston, J.E., Kim, H.I.: Adhesion, friction, and mechanical properties of functionalized alkanethiol self-assembled monolayers. Acc. Chem. Res. **35**, 547–553 (2002)
9. Cheng, H., Hu, Y.: Influence of chain ordering on frictional properties of self-assembled monolayers (SAMs) in nano-lubrication. Adv. Colloid Interface Sci. **171–172**, 53–65 (2012)

10. Ma, J.Q., Pang, C.J., Mo, Y.F., Bai, M.W.: Preparation and tribological properties of multiply-alkylated cyclopentane (MAC)–octadecyltrichlorosilane (OTS) double-layer film on silicon. Wear **263**, 1000–1007 (2007)
11. Song, S., Zhou, J., Qu, M., Yang, S., Zhang, J.: Preparation and tribological behaviors of an amide-containing stratified self-assembled monolayers on silicon surface. Langmuir **24**, 105–109 (2008)
12. Ou, J., Wang, J., Liu, S., Zhou, J., Yang, S.: Self-assembly and tribological property of a novel 3-layer organic film on silicon wafer with polydopamine coating as the interlayer. J. Phys. Chem. C **113**, 20429–20434 (2009)
13. Ou, J., Wang, J., Liu, S., Mu, B., Ren, J., Wang, H., Yang, S.: Tribology study of reduced graphene oxide sheets on silicon substrate synthesized via covalent assembly. Langmuir **26**, 15830–15836 (2010)
14. Ou, J., Wang, Y., Wang, J., Liu, S., Li, Z., Yang, S.: Self-assembly of octadecyltrichlorosilane on graphene oxide and the tribological performances of the resultant film. J. Phys. Chem. C **115**, 10080–10086 (2011)
15. Wang, Y., Pu, J., Xia, L., Ding, J., Yuan, N., Zhu, Y., Cheng, G.: Fabrication and tribological study of graphene oxide/multiply-alkylated cyclopentanes multilayer lubrication films on Si substrates. Tribol. Lett. **53**, 207–214 (2014)
16. Guo, Y.B., Wang, D.G., Liu, S.H., Zhang, S.W.: Fabrication and tribological properties of polyelectrolyte multilayers containing in situ gold and silver nanoparticles. Coll. Surf. A **417**, 1–9 (2013)
17. Guo, Y.B., Wang, D.G., Liu, S.H.: Tribologica behavior of in situ Ag nanoparticels/polyelectrolyte composite molecular deposition films. Appl. Surf. Sci. **256**, 1714–1719 (2010)
18. Zhang, S., Hu, L., Wang, H., Feng, D.: The anti-seizure effect of Ag nanoparticles additive in multialkylated cyclopentanes oil under vacuum condition. Tribol. Int. **55**, 1–6 (2012)
19. Shi, X., Xu, Z., Wang, M., Zhai, W., Yao, J., Song, S., Din, A.Q., Zhang, Q.: Tribological behavior of TiAl matrix self-lubricating composites containing silver from 25 to 800°C. Wear **303**, 486–494 (2013)
20. Yang, G., Zhang, C., Zhang, S., Yu, L., Zhang, P.: Preparation of sandwich-like self-assembled n-octanethiol film containing doped silver nanoparticles on silicon wafer and evaluation of its tribological properties. Mater. Res. Bull. **55**, 88–94 (2014)
21. Wang, Y., Biradar, A.V., Wang, G., Sharma, K.K., Duncan, C.T., Rangan, S., Asefa, T.: Controlled synthesis of water-dispersible faceted crystalline copper nanoparticles and their catalytic properties. Chem. Eur. J. **16**, 10735–10743 (2010)
22. Hu, S.W., Yang, L.W., Tian, Y., Wei, X.L., Ding, J.W., Zhong, J.X., Chu, P.K.: Simultaneous nanostructure and heterojunction engineering of graphitic carbon nitride via in situ Ag doping for enhanced photoelectrochemical activity. Appl. Catal. B: Environ. **163**, 611–622 (2015)
23. Yang, G., Yu, L., Chen, X., Zhang, P.: Hydrophobic surfaces of spin-assisted layer-by-layer assembled polyelectrolyte multilayers doped with copper nanoparticles and modified by fluoroalkylsilane. Appl. Surf. Sci. **255**, 4097–4101 (2009)
24. Ahn, H.S., Cuong, P.D., Park, S., Kim, Y.W., Lim, J.C.: Effect of molecular structure of self-assembled monolayers on their tribological behaviors in nano- and microscales. Wear **255**, 819–825 (2003)
25. Ou, J., Wang, Y., Li, C., Wang, F., Xue, M., Wang, J.: Tribological behaviors of a novel trilayer nanofilm: the influence of outer chain length and interlayer thickness. Surf. Interface Anal. **45**, 1182–1187 (2013)
26. Hoque, E., DeRose, J.A., Bhushan, B., Hipps, K.W.: Low adhesion, non-wetting phosphonate self-assembled monolayer films formed on copper oxide surfaces. Ultramicroscopy **109**, 1015–1022 (2009)
27. Bhushan, B., Kasai, T., Kulik, G., Barbieri, L., Hoffmann, P.: AFM study of perfluoroalkylsilane and alkylsilane self-assembled monolayers for anti-stiction in MEMS/NEMS. Ultramicroscopy **105**, 176–188 (2005)
28. Chambers, R.D.: Fluorine in organic chemistry. Wiley, New York (1973)
29. Yang, G.B., Chen, X.H., Zhang, Z.M., Song, S.Y., Yu, L.G., Zhang, P.Y.: Adhesion and tribological property of Cu nanoparticles-doped hydrophobic polyelectrolyte multilayers. Lubr. Sci. **24**, 313–323 (2012)
30. Álvarez-Asencio, R., Pan, J., Thormann, E., Rutland, M.W.: Tribological properties mapping: local variation in friction coefficient and adhesion. Tribol. Lett. **50**, 387–395 (2013)
31. Bhushan, B.: Handbook of micro/nano tribology, 2nd edn. CRC Press LLC, Boca Raton (1999)
32. Song, Y., Xia, Y., Liu, H., Jia, Z.: Tribological properties of alkyl and hydroxyl groups on the imidazolium tetrafluoroborate ionic liquids. Lubr. Sci. **25**, 413–427 (2013)
33. Jahanmir, S.: Chain length effects in boundary lubrication. Wear **102**, 331–349 (1985)
34. Song, S., Chu, R., Zhou, J., Yang, S., Zhang, J.: Formation and tribology study of amide-containing stratified self-assembled monolayers: influences of the underlayer structure. J. Phys. Chem. C **112**, 3805–3810 (2008)
35. Song, Y., Premachandran, N.R., Zou, M., Wang, Y.A.: Adhesion and friction properties of micro/nano-engineered superhydrophobic/hydrophobic surfaces. Thin Solid Films **518**, 3801–3807 (2010)
36. Liu, Y.H., Wang, X.K., Luo, J.B., Lu, X.C.: Fabrication and tribological properties of super-hydrophobic surfaces based on porous silicon. Appl. Surf. Sci. **255**, 9430–9438 (2009)